

Discrete Morse Theory for Computing Zigzag Persistence

Clément Maria ^{*} Hannah Schreiber [†]

July 12, 2019

Abstract

We introduce a theoretical and computational framework to use discrete Morse theory as an efficient preprocessing in order to compute zigzag persistent homology. From a zigzag filtration of complexes (X_i) , we introduce a *zigzag Morse filtration* whose complexes (\mathcal{A}_i) are Morse reductions of the original complexes (X_i) , and we prove that they both have same persistent homology. This zigzag Morse filtration generalizes the *filtered Morse complex* of Mischaikow and Nanda [40], defined for standard persistence.

The maps in the zigzag Morse filtration are forward and backward inclusions, as is standard in zigzag persistence, as well as a new type of map inducing non trivial changes in the boundary operator of the Morse complex. We study in details this last map, and design algorithms to compute the update both at the complex level and at the homology matrix level when computing zigzag persistence. The key point of our construction is that it does not require any knowledge of past and future maps of the input filtration. We deduce an algorithm to compute the zigzag persistence of a filtration that depends mostly on the number of critical cells of the complexes, and show experimentally that it performs better in practice.

1 Introduction

Persistent homology is an algebraic method that permits to characterize the evolution of the topology of a growing sequences of spaces $X_1 \subseteq \dots \subseteq X_n$, called a filtration. The theory has found many applications, especially in data analysis where it has been successfully applied to material science [34], shape classification [8, 12], or clustering [11, 14].

Filtrations can be represented with help of diagrams as follows:

$$X_1 \xrightarrow{\subseteq} X_2 \xrightarrow{\subseteq} \dots \xrightarrow{\subseteq} X_{n-1} \xrightarrow{\subseteq} X_n . \quad (1)$$

Applying a homology functor, for a coefficient field \mathbb{F} , to a filtration leads to a sequence of vector spaces — the *homology groups* $H(X_i, \mathbb{F})$ — connected by maps induced by the inclusions, known as a *persistence module*:

$$H(X_1, \mathbb{F}) \longrightarrow H(X_2, \mathbb{F}) \longrightarrow \dots \longrightarrow H(X_{n-1}, \mathbb{F}) \longrightarrow H(X_n, \mathbb{F}) . \quad (2)$$

Computing the persistent homology of a filtration (1) consists of computing the isomorphism type, known as the *interval decomposition*, of its corresponding persistence module (2).

The success of persistent homology relies on sound theoretical foundations [26, 27, 47], favorable stability properties [5, 13, 17], and fast algorithms, both theoretically [16, 18, 21, 39] and experimentally [2, 3, 6, 15], to compute the interval decomposition of an input filtration. This last effort towards better implementations has led to dramatic improvements of running times in practice, and the emergence of efficient software libraries in the field, such as *Dionysus* [41], *DIPHA* [4], *GUDHI* [36], and *Ripser* [1].

^{*}INRIA Sophia Antipolis-Méditerranée, France – clement.maria@inria.fr

[†]Graz University of Technology, Austria – hschreiber@tugraz.at – Supported by the Austrian Science Fund (FWF) grant number P 29984-N35.

Another approach to fast computation consists of preprocessing the input filtration (1) in order to drastically reduce the size of the domains X_i , while preserving the interval decomposition of the persistence module (2) [7, 25, 40, 45]. This approach has the double advantage of reducing both time and memory complexity. This goal has successfully been reached by the use of *discrete Morse theory* [25, 29, 40] (see also [19, 32]), and led to the implementation of the efficient software, such as *Perseus* [43] and *Diamorse* [24]. Additionally, noticeable successes, at the crossroad of persistence and discrete Morse theory, have been reached in the study of 3D images [45], allowing drastic improvements in memory and time performance, as well as the study of data ranging from medical imaging to material science [22, 23, 30].

Zigzag persistent homology is a generalization of persistent homology that allows the measurement and tracking of the topology of sequences of spaces that both grow and shrink, known as a *zigzag filtrations*:

$$X_1 \xrightarrow{\subseteq} X_2 \xleftarrow{\supseteq} \dots \xrightarrow{\subseteq} X_{n-1} \xleftarrow{\supseteq} X_n, \quad (3)$$

which gives a *zigzag module*, also admitting an interval decomposition:

$$H(X_1, \mathbb{F}) \longrightarrow H(X_2, \mathbb{F}) \longleftarrow \dots \longrightarrow H(X_{n-1}, \mathbb{F}) \longleftarrow H(X_n, \mathbb{F}). \quad (4)$$

The theory of zigzag persistence was introduced in [9], and theoretical [39] and practical [10, 38] algorithms have been introduced to compute it. Zigzag persistence has great applicative potential, considering it provably produces better topological information in topology inference [44], while maintaining the homology of smaller spaces X_i thanks to deletions of faces, and more generally allows a finer approach to data analysis, such as density estimation and topological bootstrapping [9].

However, computing zigzag persistence is more intricate than computing persistent homology, essentially due to the fact that the full sequence of insertions and deletions of faces is unknown, which requires the maintenance and update of heavier data structures. As a consequence, none of the optimizations of persistence algorithms adapt to the zigzag case. The relatively poor performance of zigzag persistence implementations, compared with persistent homology ones, is a major hindrance to its practical use.

Motivation and applications for zigzag persistence. We give two important applications of zigzag persistence on which we test the experimental performance of our method.

(1) *Topology inference from data points P .* A standard approach [26] consists of computing the persistent homology of the Rips complex $\mathcal{R}^\rho(P)$ on the set of points P , for an increasing threshold $\rho \geq 0$. We compute instead the zigzag persistence of oscillating Rips zigzag filtrations [44]. These filtrations add data points progressively while reducing the scale of reconstruction in order to adapt to a more and more dense set of points. Specifically,

$$\longleftarrow \dots \mathcal{R}^{\mu\varepsilon_i}(P_i) \xrightarrow{\subseteq} \mathcal{R}^{\nu\varepsilon_i}(P_i \cup \{p_{i+1}\}) \xleftarrow{\supseteq} \mathcal{R}^{\mu\varepsilon_i}(P_i \cup \{p_{i+1}\}) \longrightarrow \dots, \quad (5)$$

where $\mathcal{R}^\alpha(P)$ is the Rips complex of threshold α on points P , and ε_i a measure of the “sparsity” of the set of points $P_i := \{p_1, \dots, p_i\}$ that decreases when points are added. Finally, $0 < \mu \leq \nu$ are parameters. This filtration is known to furnish provably correct persistence diagrams, with much less noise than standard persistence [44], while naturally maintaining much smaller complexes during computation. This application is of importance in data analysis [11, 14].

(2) *Levelset persistence of images.* Given a function $f: X \rightarrow \mathbb{R}$ on a domain X , classical persistence studies the persistent homology of sublevel sets $f^{-1}(-\infty, \rho]$ for an increasing ρ . Levelset persistence [10] studies instead the zigzag persistence of the pre-images of intervals, for appropriate $s_1 \leq s_2 \leq \dots$,

$$\longleftarrow \dots f^{-1}[s_{i-1}, s_i] \xrightarrow{\subseteq} f^{-1}[s_{i-1}, s_{i+1}] \xleftarrow{\supseteq} f^{-1}[s_i, s_{i+1}] \longrightarrow \dots. \quad (6)$$

From the levelset persistence, one can recover the sublevel set persistence [10], while maintaining again much smaller structures. This application is of particular importance for medical imaging and material science [22, 23, 30].

Streaming model and memory efficiency. A main advantage of zigzag persistence is to consequently maintain much smaller complexes over the computation. To formalize this notion, we adopt a streaming model for the computation of zigzag persistence. The input is given by a stream of insertions and deletions of faces, with no knowledge of the entire zigzag filtration, and zigzag persistence is computed “on the fly”. In particular, the memory complexity of our algorithms, depends solely on the maximal size of any complex in the filtration, $\max_i |X_i|$, as opposed to the entire number of insertions and deletions of faces, which is generally much larger.

Contributions and existing results. In the spirit of [40], we introduce a preprocessing reduction of a zigzag filtration based on discrete Morse theory [29]. After introducing some background in Section 2, we introduce in Section 3 a *zigzag Morse filtration* that generalizes the filtered Morse complex [40] of standard persistence, and we prove that it has same persistent homology as the input zigzag filtration. Because of removal of cells not agreeing with the Morse decomposition, the zigzag Morse filtration contains chain maps that are not inclusions. We study the effect of those maps on the boundary operator of the Morse complex in Section 4, and design a persistence algorithm for zigzag Morse complexes in Section 5. Finally, we report on the experimental performance of the zigzag persistence algorithm for Morse complexes in Section 6.

Note that a similar approach to adapt discrete Morse theory to zigzag persistence was followed by Escobar and Hiraoka [28]. Adapting [40], they define a *global* zigzag filtered Morse complex for a zigzag filtration, and study its interval decomposition. The main limitation of their approach is that the user must know the entirety of the input zigzag filtration to compute the Morse pairing, canceling the benefit of using “small complexes” in zigzag persistence. On the contrary, our approach requires no other than local knowledge of the input zigzag filtration, and all computation are done “on the fly” in the streaming model.

2 Background

Quiver theory. Throughout this article, we fix a field $(\mathbb{F}, +, \cdot)$. An A_n -type quiver \mathcal{Q} is a directed graph:

$$\bullet_1 \longleftrightarrow \bullet_2 \longleftrightarrow \cdots \longleftrightarrow \bullet_{n-1} \longleftrightarrow \bullet_n,$$

where, by convention in this article, bidirectional arrows are either forward or backward.

An \mathbb{F} -representation of \mathcal{Q} is an assignment of a finite dimensional \mathbb{F} -vector space V_i for every node \bullet_i and an assignment of a linear map $f_i : V_i \leftrightarrow V_{i+1}$ for every arrow $\bullet_i \leftrightarrow \bullet_{i+1}$, the orientation of the map being the same as that of the arrow. We denote such a representation by $\mathbb{V} = (V_i, f_i)$. In computational topology, an \mathbb{F} -representation of an A_n -type quiver is called a *zigzag module*.

Let $\mathbb{V} = (V_i, f_i)$ and $\mathbb{W} = (W_i, g_i)$ be two \mathbb{F} -representations of a same quiver \mathcal{Q} . A *morphism of representations* $\phi : \mathbb{V} \rightarrow \mathbb{W}$ is a set of linear maps $\{\phi_i : V_i \rightarrow W_i\}_{i=1 \dots n}$ such that the diagram on the right commutes for every arrow of \mathcal{Q} . The morphism is called an *isomorphism* (denoted by \cong) if every ϕ_i is bijective.

$$\begin{array}{ccc} V_i & \xleftrightarrow{f_i} & V_{i+1} \\ \phi_i \downarrow & & \downarrow \phi_{i+1} \\ W_i & \xleftrightarrow{g_i} & W_{i+1} \end{array}$$

The *direct sum* of two \mathbb{F} -representations $\mathbb{V} = (V_i, f_i)$, $\mathbb{W} = (W_i, g_i)$, denoted by $\mathbb{V} \oplus \mathbb{W}$, is the representation of \mathcal{Q} with space $V_i \oplus W_i$ for every node \bullet_i , and with map $f_i \oplus g_i = \begin{pmatrix} f_i & 0 \\ 0 & g_i \end{pmatrix}$ for every arrow $\bullet_i \leftrightarrow \bullet_{i+1}$. An \mathbb{F} -representation \mathbb{V} is *decomposable* if it can be written as the direct sum of two non-trivial representations. It is otherwise said to be *indecomposable*.

Finally, for any $1 \leq b \leq d \leq n$, define the *interval representation* $\mathbb{I}[b; d]$ as follows:

$$\underbrace{0 \xleftarrow{0} \cdots \xleftarrow{0} 0}_{[1; b-1]} \xleftarrow{0} \underbrace{\mathbb{F} \xleftarrow{1} \cdots \xleftarrow{1} \mathbb{F}}_{[b; d]} \xleftarrow{0} \underbrace{0 \xleftarrow{0} \cdots \xleftarrow{0} 0}_{[d+1; n]},$$

where the maps 0 and $\mathbb{1}$ stand respectively for the null map and the identity map.

Theorem 1 states that every representation of an A_n -type quiver can be decomposed into interval representations, which are the indecomposables for that quiver:

Theorem 1 (Krull-Remak-Schmidt, Gabriel). *Every \mathbb{F} -representation \mathbb{V} of an A_n -type quiver can be decomposed as a direct sum of indecomposables: $\mathbb{V} \cong \mathbb{V}^1 \oplus \mathbb{V}^2 \oplus \cdots \oplus \mathbb{V}^N$, where each indecomposable \mathbb{V}^j is isomorphic to some interval representation $\mathbb{I}[b_j; d_j]$. This decomposition is unique up to permutation of the indecomposables.*

In computational topology, such algebraic decomposition of a zigzag module is called an *interval decomposition*.

Complexes and homology. We refer the reader to [35] for an introduction to general abstract complexes and their homology, and to [26] for an introduction to persistent homology.

Note that, in practice, it is common to work with specific complexes, such as simplicial or cubical complexes (as in Section 6). However, Morse reductions (introduced below) produce general complexes, which forces us to work in this general setting.

An *abstract complex* over a principal ideal domain \mathbf{D} (such as the ring of integers \mathbb{Z} or a field $\mathbb{Z}/p\mathbb{Z}$ for p prime) is a graded finite collection $X = \bigsqcup_{d \in \mathbb{Z}} X_d$ of elements, called *cells* or *faces*, together with an *incidence function* $[\cdot : \cdot]^X : X \times X \rightarrow \mathbf{D}$. The *dimension* of a cell $\sigma \in X_d$ is $\dim \sigma = d$. The incidence function satisfies, for any cells σ, τ , and μ :

$$[\sigma : \tau]^X \neq 0 \Rightarrow \dim \sigma = \dim \tau + 1 \quad \text{and} \quad \sum_{\tau \in X} [\sigma : \tau]^X \cdot [\tau : \mu]^X = 0.$$

If $[\sigma : \tau]^X \neq 0$, we call τ a *facet* of σ , and σ a *cofacet* of τ . If a cell has no cofacet, it is called *maximal*.

Standard examples of complexes are *simplicial complexes* and *cubical complexes*, with an orientation fixed on their cells. In this case, the principal ideal domain \mathbf{D} is the ring of integers \mathbb{Z} , and incidence function takes values in $\{-1, 0, 1\} \subset \mathbb{Z}$. In this work, we consider general complexes because they appear under the form of *Morse complexes*, defined later.

For a field of coefficients \mathbb{F} , we associate to a complex $(X, [\cdot : \cdot]^X)$ a *chain complex* $C(X, \mathbb{F}) = \bigoplus_d C_d(X, \mathbb{F})$, where $C_d(X, \mathbb{F})$ is the \mathbb{F} -vector space freely generated by the d -dimensional cells X_d of X . For every dimension d , the *boundary operator* $\partial_d^X : C_d(X) \rightarrow C_{d-1}(X)$ is generated by:

$$\partial_d^X \sigma = \sum_{\tau \in X_{d-1}} [\sigma : \tau]^X \cdot \tau.$$

The *d -cycles* and *d -boundaries* are $Z_d(X, \mathbb{F}) = \ker \partial_d^X$ and $B_d(X, \mathbb{F}) = \text{im } \partial_{d+1}$ respectively, and the d^{th} homology group is the quotient

$$H_d(X, \mathbb{F}) = Z_d(X, \mathbb{F}) / B_d(X, \mathbb{F}).$$

In order to simplify notations, we fix the field \mathbb{F} for the rest of the article, and remove it from notations. To put emphasis on the boundary operator, we denote a complex by (X, ∂) , where $\partial : C(X) \rightarrow C(X)$ is $\partial = \bigoplus_d \partial_d^X$. We avoid the superscript ∂^X when possible.

We denote by $\langle \cdot, \cdot \rangle : C(X) \times C(X) \rightarrow \mathbb{Z}$ the inner product on $C(X)$ making the canonical basis of cells $\{\sigma\}_{\sigma \in X}$ orthonormal. In particular, if τ is in the boundary of σ , $\langle \partial \sigma, \tau \rangle = [\sigma : \tau]^X$ in (X, ∂) . For a chain $c \in C(X)$, we say that c *contains* a cell σ , and write $\sigma \in c$, if the coefficient of σ is non-zero in c .

Definition 1. *Let X and X' be two complexes; X is included in X' if $X \subseteq X'$ as sets of cells, and $[\cdot : \cdot]^X \Big|_X = [\cdot : \cdot]^{X'}$. We also denote the inclusion of complexes by $X \subseteq X'$.*

A *standard filtration* is a finite collection of complexes with inclusion relations going one way $X_1 \subseteq X_2 \subseteq X_3 \subseteq \cdots$. A *zigzag filtration* is a collection of complexes with inclusion relations going both ways $X_1 \subseteq X_2 \supseteq X_3 \subseteq \cdots$.

Finally, a *chain map* $\psi : C(X) \rightarrow C(X')$ is a map that commutes with the boundary operators of X and X' . It induces a morphism $\psi_* : H(X) \rightarrow H(X')$ of homology groups.

Notations 1. Let X, X', Y, Y' be complexes, such that $X \subseteq X'$ and $Y \subseteq Y'$, and let $\phi: C(X) \rightarrow C(Y)$ and $\phi': C(X') \rightarrow C(Y')$ be chain maps. If the square on the right commutes, we allow ourselves to use the same notation ϕ for both ϕ and ϕ' , when there is no ambiguity on their domain and codomain.

$$\begin{array}{ccc} C(X) & \xrightarrow{\subseteq} & C(X') \\ \phi \downarrow & & \downarrow \phi' \\ C(Y) & \xrightarrow{\subseteq} & C(Y') \end{array}$$

Notations 2. By a small abuse of notations, when two complexes X and $X \cup \{\sigma\}$ differ by a single cell σ , we use the notation $X \xrightarrow{\subseteq \sigma} X \cup \{\sigma\}$ to name the chain map induced by the inclusion. When they differ by a set of cells Σ , we use the notation $X \xrightarrow{\subseteq \Sigma} X \cup \Sigma$.

Discrete Morse theory. We refer the reader to [29] for an introduction to discrete Morse theory, and to [40] for its application in persistent homology. We follow the general presentation of [40].

The incidence function of a complex induces a *face partial ordering* $<$ on X by taking the transitive closure of the relation \prec defined by

$$\tau \prec \sigma \quad \text{iff} \quad [\sigma : \tau]^X \neq 0.$$

A *partial matching* of X is a partition $X = \mathcal{A} \sqcup \mathcal{Q} \sqcup \mathcal{K}$ of the cells of the complex, together with a bijective pairing $\mathcal{Q} \leftrightarrow \mathcal{K}$, such that if $(\tau, \sigma) \in \mathcal{Q} \times \mathcal{K}$ are paired, then $\dim \sigma = \dim \tau + 1$, and $[\sigma : \tau]^X \neq 0$ is a unit in \mathbf{D} (e.g., 1 or -1 if $\mathbf{D} = \mathbb{Z}$). We call such pair of cells a *Morse pair*. We denote the bijection $\omega: \mathcal{Q} \rightarrow \mathcal{K}$, such that Morse pairs are of the form $(\tau, \omega(\tau))$.

Call \mathcal{H} the *oriented Hasse diagram* of $(X, <)$ where arrows are oriented downwards (i.e., from higher to lower dimensions), except for the arrows between cells of Morse pairs $(\tau, \sigma) \in \mathcal{Q} \times \mathcal{K}$, oriented upwards.

A *Morse matching* of a complex X is a partial matching that induces an *acyclic* oriented Hasse diagram \mathcal{H} for X . We denote a Morse matching with a partition $\mathcal{A} \sqcup \mathcal{Q} \sqcup \mathcal{K}$ and pairing $\omega: \mathcal{Q} \rightarrow \mathcal{K}$ by $(\mathcal{A}, \mathcal{Q}, \mathcal{K}, \omega)$. Note that a Morse matching can also be defined on a subset Σ of cells of a complex X . By convention, we denote $(\mathcal{A}, \mathcal{Q}, \mathcal{K}, \omega)$ Morse matchings for a *complex*, and $(\hat{\mathcal{A}}, \hat{\mathcal{Q}}, \hat{\mathcal{K}}, \hat{\omega})$ Morse matchings for a *set of faces* not forming a complex.

In a complex with a Morse matching, a *gradient path* between a $d+1$ -dimensional cell ν and a d -dimensional cell μ is a simple directed path in \mathcal{H} from ν to μ alternating between d and $d+1$ -dimensional cells¹. Every gradient path γ is consequently simple and of the form:

$$\gamma = \nu \begin{array}{c} \searrow \\ \tau_1 \end{array} \begin{array}{c} \nearrow \\ \omega(\tau_1) \end{array} \begin{array}{c} \searrow \\ \tau_2 \end{array} \begin{array}{c} \nearrow \\ \omega(\tau_2) \end{array} \dots \begin{array}{c} \searrow \\ \tau_r \end{array} \begin{array}{c} \nearrow \\ \omega(\tau_r) \end{array} \begin{array}{c} \searrow \\ \mu \end{array} \quad \begin{array}{l} \dim d+1 \\ \dim d. \end{array} \quad (7)$$

We denote by $\Gamma(\nu, \mu)$ the set of all distinct gradient paths from ν to μ , and we define for every path γ (with the notations of Diagram (7)) its *multiplicity* $m(\gamma)$:

$$m(\gamma) := [\nu : \tau_1]^X \cdot (-1)^r \cdot \prod_{i=1}^r \left([\omega(\tau_i) : \tau_i]^X \right)^{-1} \cdot \prod_{i=1}^{r-1} [\omega(\tau_i) : \tau_{i+1}]^X \cdot [\omega(\tau_r) : \mu]^X$$

and $m(\gamma) = [\nu : \mu]^X$ for the one-edge path $\gamma = (\nu, \mu)$, if it exists. In other words, the multiplicity is the product of incidences for downward arrows, times the product of minus the inverse of incidences for upward arrows in the path.

Given a complex X and a Morse matching $(\mathcal{A}, \mathcal{Q}, \mathcal{K}, \omega)$, the *Morse complex* $(\mathcal{A}, \partial^{\mathcal{A}})$ associated to the matching is the complex based on the cells of \mathcal{A} , called the *critical cells*, with incidence function $[\cdot : \cdot]^{\mathcal{A}}: \mathcal{A} \times \mathcal{A} \rightarrow \mathbf{D}$ defined, for two critical cells $\nu, \mu \in \mathcal{A}$, by

$$[\nu : \mu]^{\mathcal{A}} := \sum_{\gamma \in \Gamma(\nu, \mu)} m(\gamma).$$

¹ Note that our definition differs from the original reference [29], where gradient paths connect cells of same dimension.

The dimension of a critical cell σ in \mathcal{A} is the same as the dimension of σ in the original complex X . We denote the set of d -dimensional cells of \mathcal{A} by \mathcal{A}_d . As a complex, the boundary operator of \mathcal{A} is defined, for $\sigma \in \mathcal{A}_d$ a critical cell of dimension d , by

$$\partial_d^{\mathcal{A}} : \mathcal{A}_d \rightarrow \mathcal{A}_{d-1}, \quad \text{such that} \quad \partial_d^{\mathcal{A}} \tau = \sum_{\mu \in \mathcal{A}_{d-1}} [\nu : \mu]^{\mathcal{A}} \cdot \mu.$$

By a small abuse of notation, we refer to X and \mathcal{A} as chain complexes and write $H(X)$ and $H(\mathcal{A})$ for their homology, provided there is no ambiguity in the definition of their incidence function and boundary maps.

We finally have the fundamental theorem of discrete Morse theory,

Theorem 2 (Forman [29]). *A complex (X, ∂^X) and a Morse complex $(\mathcal{A}, \partial^{\mathcal{A}})$, for a Morse matching $(\mathcal{A}, \mathcal{Q}, \mathcal{K}, \omega)$ of X , have isomorphic homology groups².*

Persistent homology and discrete Morse theory. We refer the reader to [40] for the study of the (standard) persistent homology of discrete Morse complexes.

Persistent homology is the study of persistent modules induced by filtrations. Let $X_1 \subseteq \dots \subseteq X_n$ be a filtration of complexes. A *standard Morse filtration* (called *filtered Morse complex* in [40]) for this filtration is a collection of Morse matchings $(\mathcal{A}_i, \mathcal{Q}_i, \mathcal{K}_i, \omega_i)_{i=1 \dots n}$ for each X_i , with Morse complex $(\mathcal{A}_i, \partial^{\mathcal{A}_i})$ on the critical cells, and Morse pairs $\omega_i : \mathcal{K}_i \xrightarrow{\text{bij.}} \mathcal{Q}_i$, satisfying:

$$\mathcal{A}_i \subseteq \mathcal{A}_{i+1}, \quad \mathcal{Q}_i \subseteq \mathcal{Q}_{i+1}, \quad \mathcal{K}_i \subseteq \mathcal{K}_{i+1}, \quad \omega_{i+1}|_{\mathcal{Q}_i} = \omega_i, \quad \partial^{\mathcal{A}_{i+1}}|_{\mathcal{A}_i} = \partial^{\mathcal{A}_i}. \quad (8)$$

A filtered Morse complex consequently forms a filtration $\mathcal{A}_1 \subseteq \dots \subseteq \mathcal{A}_n$ of Morse complexes connected by inclusions. It induces naturally a persistence module:

$$H(\mathcal{A}_1, \mathbb{F}) \longrightarrow H(\mathcal{A}_2, \mathbb{F}) \longrightarrow \dots \longrightarrow H(\mathcal{A}_{n-1}, \mathbb{F}) \longrightarrow H(\mathcal{A}_n, \mathbb{F}).$$

Forman's isomorphism between homology groups of complexes and Morse complexes extends to persistent homology groups within this framework. Specifically,

Theorem 3 (Forman [29], Mischaikow and Nanda [40]). *Let $(\mathcal{A}_i, \mathcal{Q}_i, \mathcal{K}_i, \omega_i)_{i=1 \dots n}$ be a standard Morse filtration for a filtration $X_1 \subseteq \dots \subseteq X_n$. There exist collections of chain maps $(\psi_i : C(X_i) \rightarrow C(\mathcal{A}_i))_{i=1 \dots n}$ and $(\varphi_i : C(\mathcal{A}_i) \rightarrow C(X_i))_{i=1 \dots n}$ for which the following diagrams commute for every i :*

$$\begin{array}{ccc} C(X_i) & \xrightarrow{\subseteq} & C(X_{i+1}) \\ \psi_i \downarrow & & \downarrow \psi_{i+1} \\ C(\mathcal{A}_i) & \xrightarrow{\subseteq} & C(\mathcal{A}_{i+1}) \end{array} \qquad \begin{array}{ccc} C(X_i) & \xrightarrow{\subseteq} & C(X_{i+1}) \\ \varphi_i \uparrow & & \uparrow \varphi_{i+1} \\ C(\mathcal{A}_i) & \xrightarrow{\subseteq} & C(\mathcal{A}_{i+1}) \end{array}$$

and φ_i and ψ_i induce isomorphisms at the homology level, that are inverses of each other. Consequently, these maps induce isomorphisms between the persistent modules of the filtration and the Morse filtration.

Without expressing them explicitly, we use the following properties of the map ψ (see [40] for explicit formulations):

Properties 1. *Let X be a complex with a Morse matching $(\mathcal{A}, \mathcal{Q}, \mathcal{K}, \omega)$. The chain map $\psi : C(X) \rightarrow C(\mathcal{A})$ can be expressed as the composition of elementary chain maps over all Morse pairs (τ, σ) , taken in an arbitrary order,*

$$\psi = \prod_{(\tau, \sigma), \text{ s.t. } \sigma = \omega(\tau)} \psi_{\tau, \sigma},$$

²In fact, the complexes are *homotopy equivalent*.

where $\psi_{\tau,\sigma}: C(X') \rightarrow C(X' \setminus \{\tau,\sigma\})$ is defined on a “partially reduced” complex X' to $X' \setminus \{\tau,\sigma\}$, with incidence functions induced by the partial matching. More specifically, X' is a Morse complex of X for a matching $(\mathcal{A}', \mathcal{Q}', \mathcal{K}', \omega')$, such that $\mathcal{Q}' \subseteq \mathcal{Q}$, $\mathcal{K}' \subseteq \mathcal{K}$, and the restriction of ω to \mathcal{Q}' is equal to ω' . The complex $X' \setminus \{\tau,\sigma\}$ is the Morse complex of X with one more Morse pair (τ,σ) . The set of Morse pairs already considered in $\mathcal{Q}' \times \mathcal{K}'$ is dependent of the order in which the maps are composed.

The map $\psi_{\tau,\sigma}$ satisfies:

- (1) $\psi_{\tau,\sigma}(\sigma) = 0$,
- (2) $\psi_{\tau,\sigma}(\tau)$ is a linear combination of facets of σ in X' , and
- (3) $\psi_{\tau,\sigma}(\mu) = \mu$ for all $\mu \neq \sigma, \tau$.

Similarly, the map $\varphi: C(\mathcal{A}) \rightarrow C(X)$ can be decomposed into

$$\varphi = \prod_{(\tau,\sigma), \text{ s.t. } \sigma=\omega(\tau)} \varphi_{\tau,\sigma},$$

such that $\varphi_{\tau,\sigma}: C(X' \setminus \{\tau,\sigma\}) \rightarrow C(X')$ and $\psi_{\tau,\sigma}: C(X') \rightarrow C(X' \setminus \{\tau,\sigma\})$ induce isomorphisms at the homology level, that are inverse of each other (defined on the appropriate domain and codomain).

3 Zigzag Morse filtration and persistence

For a zigzag filtration of complexes \mathcal{F} , we introduce in this article a canonical zigzag filtration \mathcal{M} of Morse complexes admitting the same persistent homology.

3.1 Zigzag Morse filtration

Without loss of generality, consider the zigzag filtration

$$\overline{\mathcal{F}} := \overline{X}_1 \xleftarrow{\Sigma_1} \overline{X}_2 \xrightarrow{\Sigma_2} \dots \xleftarrow{\Sigma_{2k-1}} \overline{X}_{2k-1} \xrightarrow{\Sigma_{2k}} \overline{X}_{2k}, \quad (9)$$

where the \overline{X}_i are complexes, $\overline{X}_1 = \overline{X}_{2k} = \emptyset$, and the i^{th} arrow is an inclusion, either forward (i odd) or backward (i even), where complexes \overline{X}_i and \overline{X}_{i+1} differ by a set of cells Σ_i (possibly empty). We now further decompose $\overline{\mathcal{F}}$.

Atomic operations. For each forward arrow $\bullet_i \longrightarrow \bullet_{i+1}$, i odd, let $(\hat{\mathcal{A}}_i, \hat{\mathcal{Q}}_i, \hat{\mathcal{K}}_i, \hat{\omega}_i)$ be a Morse matching of the set of cells Σ_i .

Because Morse matchings are acyclic, there exists a total ordering of the cells of Σ_i , compatible with the face partial ordering of Σ_i , such that paired cells in $(\hat{\mathcal{A}}_i, \hat{\mathcal{Q}}_i, \hat{\mathcal{K}}_i, \hat{\omega}_i)$ are consecutive with regard to that order. We can consequently decompose a forward inclusion $\overline{X}_i \subseteq \overline{X}_{i+1}$ into a sequence of inclusions of a single critical cell $\sigma \in \hat{\mathcal{A}}_i$, and of inclusions of a single Morse pair of cells $(\tau, \sigma) \in \hat{\mathcal{Q}}_i \times \hat{\mathcal{K}}_i$, with $\sigma = \hat{\omega}_i(\tau)$.

For every backward arrow $\bullet_i \longleftarrow \bullet_{i+1}$, i even, the Morse matchings $(\hat{\mathcal{A}}_j, \hat{\mathcal{Q}}_j, \hat{\mathcal{K}}_j, \hat{\omega}_j)$, for smaller odd indices $j < i$, induce a Morse matching on the cells of X_i . To avoid ambiguity, if a cell is reinserted in the filtration after being removed it is considered as a different element. By restriction, they consequently induce a valid Morse matching on all cells of Σ_i , except on those cells $\sigma \in \Sigma_i$ that form a Morse pair (τ, σ) , with $\tau \notin \Sigma_i$. We decompose backward arrows into a sequence of removals of a single critical cell, of removals of a single Morse pair of cells, and of removals of a non-critical cell σ , without its paired cell $\tau \notin \Sigma_i$.

In summary, given an input filtration $\overline{\mathcal{F}}$ as above, and the Morse matchings $(\hat{\mathcal{A}}_i, \hat{\mathcal{Q}}_i, \hat{\mathcal{K}}_i, \hat{\omega}_i)$, we defined an *atomic* zigzag filtration

$$\mathcal{F} := (\emptyset =) X_1 \longleftarrow X_2 \longrightarrow \dots \longleftarrow X_{n-1} \longrightarrow X_n (= \emptyset),$$

where all arrows are of the following three types:

$$X \xleftarrow{\sigma} X' \quad (10) \quad X \xleftarrow{\{\tau, \sigma\}} X' \quad (11) \quad X \xrightarrow{\mathbb{1}} X \xleftarrow{\sigma} X \setminus \{\sigma\} \quad (12)$$

where σ is in each case a maximal cell in X , Diagrams (10) and (11) are forward or backward insertions of a critical cell or a Morse pair (τ, σ) of cells, respectively, and Diagram (12) is the removal of the cell σ from a Morse pair (τ, σ) , where the cell τ is not removed. The identity arrow in this last diagram is a technicality that is clarified later. Naturally, one can recover the persistent homology of the zigzag filtration $\overline{\mathcal{F}}$ from the one of \mathcal{F} . We work with \mathcal{F} for the rest of the article.

Morse filtration. Given a zigzag filtration $\overline{\mathcal{F}}$, Morse matchings $(\mathcal{A}_i, \mathcal{Q}_i, \mathcal{K}_i, \omega_i)$, and an associated atomic filtration \mathcal{F} as above, we define a *zigzag Morse filtration*

$$\mathcal{M} := (\emptyset =) \mathcal{A}_1 \longleftrightarrow \mathcal{A}_2 \longleftrightarrow \dots \longleftrightarrow \mathcal{A}_{n-1} \longleftrightarrow \mathcal{A}_n (= \emptyset),$$

of Morse complexes $(\mathcal{A}_i, \partial^{\mathcal{A}_i})$ of the complexes (X_i, ∂^{X_i}) of \mathcal{F} inductively. Note that the maps of the zigzag Morse filtration are not all inclusions. Specifically, for a critical cell σ in both X_i and X_{i+1} , in general $\partial^{\mathcal{A}_i}(\sigma) \neq \partial^{\mathcal{A}_{i+1}}(\sigma)$.

All X_1, X_n, \mathcal{A}_1 and \mathcal{A}_n are empty complexes. The zigzag Morse filtration is constructed inductively for the insertion of a critical cell (Diagram (10)) and the insertion of a Morse pair (Diagram (11)) as for standard Morse filtrations [40]:

$$\begin{array}{ccc} C(X) \xrightarrow{\sigma'} C(X \cup \{\sigma'\}) & & C(X) \xrightarrow{\{\tau, \sigma\}} C(X \cup \{\tau, \sigma\}) \\ \psi \downarrow & & \downarrow \psi \\ C(\mathcal{A}) \xrightarrow{\sigma'} C(\mathcal{A} \cup \{\sigma'\}) & & C(\mathcal{A}) \xrightarrow{\mathbb{1}} C(\mathcal{A}), \end{array} \quad (13)$$

where all horizontal arrows are inclusions of complexes, and in particular the boundary maps of \mathcal{A} and $\mathcal{A} \cup \{\sigma'\}$ are equal when restricted to the cells of \mathcal{A} . The removal of critical cells and Morse pairs is symmetrical. The chain maps ψ and $\psi_{\tau, \sigma}$ are the ones of Theorem 3 and Properties 1, and are used later.

For the removal of a non-critical cell σ without its paired cell τ (Diagram (12)), which is specific to zigzag persistence, the Morse filtration is constructed with:

$$\begin{array}{ccc} C(X) \xrightarrow{\mathbb{1}} C(X) \xleftarrow{\sigma} C(X \setminus \{\sigma\}) & & \\ \psi_{\tau, \sigma} \circ \psi \downarrow & & \downarrow \psi \\ C(\mathcal{A}, \partial) \xrightarrow{\varphi_{\tau, \sigma}} C(\mathcal{A} \cup \{\tau, \sigma\}, \partial') \xleftarrow{\sigma} C(\mathcal{A} \cup \{\tau\}, \partial') & & \end{array} \quad (14)$$

The main technicality is that the boundary maps ∂ and ∂' differ in a non trivial way, that we study in Section 4. The map ∂'' is equal to the restriction of ∂' to the critical cells $\mathcal{A} \cup \{\tau\}$ (the right arrow is a backward inclusion of complexes). The chain maps $\psi_{\tau, \sigma}$ and $\varphi_{\tau, \sigma}$ are the ones from Theorem 3 and Properties 1, and ψ is the compositions of all maps $\psi_{\mu, \omega(\mu)}$ over the Morse pairs $(\mu, \omega(\mu))$ of the Morse matching of X , except the pair (τ, σ) . We give an example of zigzag Morse filtration in Figure 1.

Diagrams (13) are studied in [40]. We now focus on the study of Diagram (14).

Remark 1. Note that a key point for the proofs of theorems in [40] is that filtered Morse complexes in standard persistence satisfy $(\mathcal{A}_i, \partial) \subset (\mathcal{A}_{i+1}, \partial)$. This fact also allows the standard persistent homology algorithm [27, 47] to work directly for filtered Morse complexes. This property is not satisfied by zigzag Morse filtrations, which explains why our approach is more atomic than the one of [40] (see Section 3.2), and that we have to design a new homology matrix algorithm to implement operation (14) (see Sections 4 and 5).

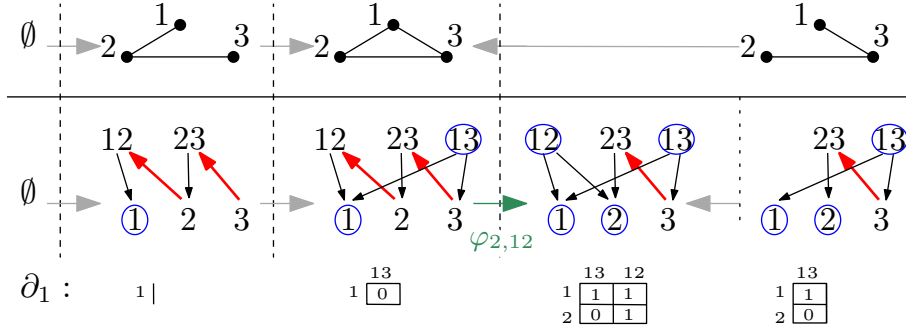


Figure 1: Zigzag filtration (top) and its Morse filtration (bottom), given by Hasse diagrams and (Morse) boundary maps. Upward arrows in Hasse diagrams represent Morse matchings, critical faces are circled. Note that the rightmost operation illustrates Diagram (14), with a non trivial modification of $\partial_1(\{1, 3\})$.

3.2 Isomorphism of zigzag modules

Theorem 3 implies that the atomic operations of Diagrams (13) induce commuting diagrams in homology, with vertical maps being isomorphisms as proved in [40]:

Lemma 4. *Let X be a complex and $(\mathcal{A}, \mathcal{Q}, \mathcal{K}, \omega)$ a Morse complex obtained from X . Let σ' be a cell, and (τ, σ) a Morse pair, such that $(\mathcal{A} \cup \{\sigma'\}, \mathcal{Q}, \mathcal{K})$ and $(\mathcal{A}, \mathcal{Q} \cup \{\tau\}, \mathcal{K} \cup \{\sigma\})$ are valid Morse complexes. Then there exist isomorphisms ψ_* and $(\psi_{\tau, \sigma})_*$ such that the following diagrams commute:*

$$\begin{array}{ccc}
 H(X) \xrightarrow{\sigma'_*} H(X \cup \{\sigma'\}) & & H(X) \xrightarrow{\sigma_* \circ \tau_*} H(X \cup \{\tau, \sigma\}) \\
 \psi_* \downarrow & & \psi_* \downarrow \\
 H(\mathcal{A}) \xrightarrow{\sigma'_*} H(\mathcal{A} \cup \{\sigma'\}) & & H(\mathcal{A}) \xrightarrow{1} H(\mathcal{A}) \\
 & & \downarrow (\psi_{\tau, \sigma})_* \circ \psi_*
 \end{array}$$

where σ'_* and $\sigma_* \circ \tau_*$ are the maps induced at homology level by the insertion of σ' and $\{\tau, \sigma\}$ respectively. The maps ψ_* and $(\psi_{\tau, \sigma})_*$ are the isomorphisms induced by chain maps ψ and $\psi_{\tau, \sigma}$ of discrete Morse theory (see Theorem 3).

We prove the following lemma, which is specific to our zigzag Morse filtration.

Lemma 5. *Let X be a complex and $(\mathcal{A}, \mathcal{Q}, \mathcal{K}, \omega)$ a Morse complex obtained from X . Let σ be a maximal cell of X not in \mathcal{A} , which therefore forms a Morse pair with a cell τ , $[\sigma : \tau]^X \neq 0$. There exist isomorphisms ψ_* , $(\psi_{\tau, \sigma})_*$, and $(\varphi_{\tau, \sigma})_*$ such that the following diagram commutes:*

$$\begin{array}{ccc}
 H(X) \xrightarrow{1} H(X) \xleftarrow{\sigma_*} H(X \setminus \{\sigma\}) \\
 (\psi_{\tau, \sigma})_* \circ \psi_* \downarrow & & \downarrow \psi_* \\
 H(\mathcal{A}) \xrightarrow{(\varphi_{\tau, \sigma})_*} H(\mathcal{A} \cup \{\tau, \sigma\}) \xleftarrow{\sigma_*} H(\mathcal{A} \cup \{\tau\})
 \end{array}$$

where σ_* is the map induced at homology level by the removal of σ . The maps ψ_* , $(\psi_{\tau, \sigma})_*$, and $(\varphi_{\tau, \sigma})_*$ are the isomorphisms induced at homology level by, respectively, the chain maps ψ , $\psi_{\tau, \sigma}$, and $\varphi_{\tau, \sigma}$ of discrete Morse theory (see Theorem 3).

Proof. Apply the homology functor to Diagram (14). The right square commutes, being induced by horizontal inclusions. Because the maps induced at homology level by $\psi_{\tau, \sigma}$ and $\varphi_{\tau, \sigma}$ are isomorphisms, inverse of each other (see Theorem 3), we get $(\varphi_{\tau, \sigma})_* \circ (\psi_{\tau, \sigma})_* \circ \psi_* = \psi_*$ and the left square commutes. \square

We conclude,

Theorem 6. *The zigzag filtrations \mathcal{F} and \mathcal{M} have same persistent homology.*

Proof. Applying the homology functor to \mathcal{F} and \mathcal{M} , we get the zigzag modules

$$\begin{array}{ccccccc} H(\mathcal{F}) : & & H(X_0) & \longleftrightarrow & H(X_1) & \longleftrightarrow & \cdots & \longleftrightarrow & H(X_m) \\ & & \downarrow \psi_*^0 & & \downarrow \psi_*^1 & & & & \downarrow \psi_*^m \\ H(\mathcal{M}) : & & H(\mathcal{A}_0) & \longleftrightarrow & H(\mathcal{A}_1) & \longleftrightarrow & \cdots & \longleftrightarrow & H(\mathcal{A}_m) \end{array}$$

where, by construction, every \mathcal{A}_i is a Morse complex of X_i , and the ψ_*^i are the isomorphisms induced by the chain maps $\psi^i: C(X_i) \rightarrow C(\mathcal{A}_i)$, connecting a complex and its Morse reduction (Theorem 3). By Theorem 3 and Lemma 5, all squares commute and are compatible with each other, and the (ψ_*^i) define an isomorphism of zigzag modules. \square

4 Boundary of the Morse complex

Referring to Diagram (14), let X be a complex with incidence function $[\cdot : \cdot]^X$, together with a Morse matching $(\mathcal{A}, \mathcal{Q}, \mathcal{K}, \omega)$, inducing an orientation of the Hasse diagram \mathcal{H} of the complex, and a Morse complex (\mathcal{A}, ∂) .

In this section, we track the evolution of the boundary operators in Morse complexes under the evaluation of the map $\varphi_{\tau, \sigma}: (\mathcal{A}, \partial) \rightarrow (\mathcal{A} \cup \{\tau, \sigma\}, \partial')$ from Diagram (14). Both complexes are Morse complexes of the same X , whose matchings differ by exactly one pair (τ, σ) , i.e., the Morse partition of complex $\mathcal{A} \cup \{\tau, \sigma\}$ is $(\mathcal{A} \cup \{\tau, \sigma\}) \sqcup (\mathcal{Q} \setminus \{\tau\}) \sqcup (\mathcal{K} \setminus \{\sigma\})$. We denote this last complex by $(\mathcal{A}', \partial')$, with incidence function $[\cdot : \cdot]^{\mathcal{A}'}$ in the following. We prove:

Lemma 7. *Let ν be a cell of the complex (\mathcal{A}, ∂) . Then, in the complex $(\mathcal{A}', \partial')$,*

$$\partial'(\nu) = \partial(\nu) + \left([\sigma : \tau]^X\right)^{-1} [\nu : \tau]^{\mathcal{A}'} \cdot \partial'\sigma. \quad (15)$$

Proof. First, note that σ is maximal in X , and so it is maximal in $\mathcal{A} \cup \{\tau, \sigma\}$.

Let \mathcal{H} and \mathcal{H}' be the Hasse diagrams of X induced by the Morse matchings of \mathcal{A} and \mathcal{A}' , respectively. Because the matchings differ by a single Morse pair (τ, σ) , \mathcal{H} and \mathcal{H}' only differ by the orientation of the edge $\tau \leftrightarrow \sigma$.

For a critical cell $\nu \in \mathcal{A}$, we have:

$$\partial\nu = \sum_{\substack{\mu \in \mathcal{A} \\ \gamma \in \Gamma(\nu, \mu)}} m(\gamma) \cdot \mu = \underbrace{\sum_{\substack{\mu \in \mathcal{A}, \\ \gamma \in \Gamma_{\tau \rightarrow \sigma}(\nu, \mu)}} m(\gamma) \cdot \mu}_{(*)} + \underbrace{\sum_{\substack{\mu \in \mathcal{A}, \\ \gamma \in \Gamma_{\tau \leftrightarrow \sigma}(\nu, \mu)}} m(\gamma) \cdot \mu}_{\partial'\nu - [\nu : \tau]^{\mathcal{A}'} \cdot \tau}$$

where $\Gamma_{\tau \rightarrow \sigma}(\nu, \mu)$ are the gradient paths from ν to μ in \mathcal{H} containing the upward arrow $\tau \rightarrow \sigma$, and $\Gamma_{\tau \leftrightarrow \sigma}(\nu, \mu)$ are the ones not containing it. Assume τ is of dimension d , and σ of dimension $d+1$.

Because σ is critical in \mathcal{A}' , it has no ingoing arrow from cells of dimension d in \mathcal{H}' . Consequently, $\Gamma_{\tau \rightarrow \sigma}(\nu, \mu)$ contains exactly all gradient paths from ν to $\mu \neq \tau$ in \mathcal{H}' . Hence, the sum over $\Gamma_{\tau \rightarrow \sigma}(\nu, \mu)$, for $\mu \in \mathcal{A}$, gives $\partial'\nu - [\nu : \tau]^{\mathcal{A}'} \cdot \tau$. Note that σ cannot appear in $\partial'\nu$ because σ is maximal by hypothesis.

Now, studying the left term $(*)$, and splitting gradient paths passing through edge (τ, σ) , then factorizing, we get

$$\begin{aligned} (*) &= \sum_{\substack{\mu \in \mathcal{A}, \\ \gamma_1 \in \Gamma(\nu, \tau), \\ \gamma_2 \in \Gamma(\sigma, \mu)}} m(\gamma_1) \cdot \left(-[\sigma : \tau]^X\right)^{-1} m(\gamma_2) \cdot \mu \\ &= -\left([\sigma : \tau]^X\right)^{-1} \underbrace{\sum_{\mu \in \mathcal{A}} \left(\sum_{\gamma_2 \in \Gamma(\sigma, \mu)} m(\gamma_2) \cdot \mu \right)}_{(*)_2} \cdot \underbrace{\left(\sum_{\gamma_1 \in \Gamma(\nu, \tau)} m(\gamma_1) \right)}_{(*)_1}. \end{aligned}$$

The sum (\star_1) over $\Gamma(\nu, \tau)$ is independent of μ , and equal to $[\nu : \tau]^{\mathcal{A}'}$ by definition.

Because τ is critical in \mathcal{A}' , it has no outgoing arrow towards cells of dimension $d + 1$ in \mathcal{H}' . Consequently, $\Gamma(\sigma, \mu)$ contains exactly all gradient paths from σ to μ in \mathcal{H}' , where $\mu \neq \tau$. Hence, the sum (\star_2) over $\Gamma(\sigma, \mu)$ gives $\partial' \sigma - [\sigma : \tau]^X \cdot \tau$.

Finally, putting terms together, the following allows us to conclude:

$$\begin{aligned} \partial \nu &= \left(\partial' \nu - [\nu : \tau]^{\mathcal{A}'} \cdot \tau \right) - \frac{[\nu : \tau]^{\mathcal{A}'}}{[\sigma : \tau]^X} \left(\partial' \sigma - [\sigma : \tau]^X \cdot \tau \right) \\ &= \partial' \nu - \left([\sigma : \tau]^X \right)^{-1} [\nu : \tau]^{\mathcal{A}'} \partial' \sigma. \end{aligned}$$

□

5 Persistence algorithm for zigzag Morse complexes

We describe in this section, our implementation of the algorithm to compute the persistence diagram of a zigzag Morse filtration as defined in Section 3. It consists of adapting the zigzag persistence algorithm [38], used in our experiments, to our Morse framework, relying on the results of Sections 3 and 4. Our approach could be adapted for implementing algorithm [9, 10].

5.1 Zigzag Persistence algorithm

We first recall the algorithms for computing zigzag persistence.

Existing zigzag persistence algorithms. There are currently two practical³ approaches to compute zigzag persistent homology [9, 10, 38]. They can both be formulated in a unified framework [37]. Given an input zigzag filtration:

$$X_1 \xrightarrow{\subseteq} X_2 \xleftarrow{\supseteq} \cdots \xrightarrow{\subseteq} X_{n-1} \xleftarrow{\supseteq} X_n, \quad (16)$$

both algorithms are iterative. At step i of the computation, they maintain a homology basis of $H(X_i)$ that is *compatible* (defined later) with the interval decomposition of the zigzag module associated to a zigzag filtration of the form

$$X_1 \longleftrightarrow X_2 \longleftrightarrow \cdots \longleftrightarrow X_i \longleftrightarrow X'_{i+1} \longleftrightarrow \cdots \longleftrightarrow X'_{i+m-1} \longleftrightarrow X'_{i+m}, \quad (17)$$

The first i complexes and $i - 1$ maps in (16) and (17) are identical, and the remaining complexes and maps of (17) are algorithm dependent. Both algorithms consist of updating a homology basis in order to maintain its compatibility when operating (a subset of) the following three local transformations of the zigzag filtration/module in sequence:

$$\leftrightarrow X \begin{array}{c} \xrightarrow{\sigma} X \cup \{\sigma\} \\ \searrow \quad \swarrow \\ \quad X \end{array} \begin{array}{c} \xleftarrow{\sigma} \\ \swarrow \quad \searrow \\ \quad X \end{array} \leftrightarrow, \quad (18)$$

$$\leftrightarrow X \begin{array}{c} \xleftarrow{\sigma} X \cup \{\sigma\} \\ \swarrow \quad \searrow \\ \quad X \end{array} \begin{array}{c} \xrightarrow{\sigma} \\ \swarrow \quad \searrow \\ \quad X \end{array} \leftrightarrow, \quad (19)$$

$$\leftrightarrow X \cup \{\sigma, \tau\} \begin{array}{c} \xleftarrow{\sigma} X \cup \{\tau\} \\ \swarrow \quad \searrow \\ \quad X \end{array} \begin{array}{c} \xrightarrow{\tau} \\ \swarrow \quad \searrow \\ \quad X \end{array} \leftrightarrow, \quad (20)$$

where each arrow represents the insertion of a cell. These transformations are called *reflection diamonds* for (18) and (19), and *transposition diamonds* for (20), and their effect on the interval decomposition of the zigzag module have been characterized for general zigzag filtrations of complexes in [37, 38].

We now focus on the algorithm introduced in [38] that we use in our experiments.

³ Putting aside [39], which is essentially of theoretical nature.

The zigzag algorithm of [38]. Let $\mathcal{F} : X_1 \longleftrightarrow X_2 \longleftrightarrow \dots \longleftrightarrow X_n$ be the input zigzag filtration, where *all* arrows are forward or backward inclusions of a single cell. Let \mathcal{F}_j be:

$$X_1 \longleftrightarrow X_2 \longleftrightarrow \dots \longleftrightarrow X_j \xleftarrow{\sigma_1} X'_{j+1} \xleftarrow{\sigma_2} \dots \xleftarrow{\sigma_{m-1}} X'_{j+m-1} \xleftarrow{\sigma_m} X'_{j+m} = \emptyset.$$

For indices $1 \leq p \leq q \leq n$, denote by $\mathcal{Z}[p; q]$ the restriction of a filtration \mathcal{Z} to spaces of indices $i \in [p; q]$, and maps between them.

Passing from filtration \mathcal{F}_j to filtration \mathcal{F}_{j+1} using reflection and transposition diamonds consists of the following:

(1) If $X_j \xrightarrow{\sigma} X_{j+1}$ is forward in \mathcal{F} , define \mathcal{F}_{j+1} to be

$$X_1 \longleftrightarrow \dots \longleftrightarrow X_j \xrightarrow{\sigma} X_{j+1} \xleftarrow{\sigma} X_j \xleftarrow{\sigma_1} X'_{j+1} \xleftarrow{\sigma_2} \dots \xleftarrow{\sigma_m} X'_{j+m} = \emptyset.$$

Considering $\overline{\mathcal{F}}_j$ to be \mathcal{F}_j with two extra identity arrows,

$$\overline{\mathcal{F}}_j : X_1 \longleftrightarrow \dots \longleftrightarrow X_j \xrightarrow{\mathbb{1}} X_j \xleftarrow{\mathbb{1}} X_j \xleftarrow{\sigma_1} X'_{j+1} \xleftarrow{\sigma_2} \dots \xleftarrow{\sigma_m} X'_{j+m} = \emptyset,$$

we have that $\overline{\mathcal{F}}_j$ and \mathcal{F}_{j+1} are related by a reflection diamond (Diagram (18)) at X_j . Studying the effect of a reflection diamond on homology, algorithm [38] updates a homology matrix (defined below in this framework) at X_j , compatible with \mathcal{F}_j (and also $\overline{\mathcal{F}}_j$), into a homology matrix at X_{j+1} , compatible with \mathcal{F}_{j+1} defined above.

(2) If $X_j \xleftarrow{\sigma} X_{j+1}$ is backward in \mathcal{F} , there exists an index ℓ such that $\sigma = \sigma_\ell$ in the part $\mathcal{F}_j[j; j+m]$ of the filtration \mathcal{F}_j . Define \mathcal{F}_{j+1} to be

$$\dots X_j \xleftarrow{\sigma_\ell = \sigma} X_{j+1} \xleftarrow{\sigma_1} X'_{j+1} \setminus \{\sigma\} \dots \xleftarrow{\sigma_{\ell-2}} X'_{j+\ell-2} \setminus \{\sigma\} \xleftarrow{\sigma_{\ell-1}} X'_{j+\ell} \xleftarrow{\sigma_{\ell+1}} \dots,$$

where the removal of $\sigma = \sigma_\ell$ has been moved all the way up to X_j . This can be attained by applying successively transposition diamonds (Diagram (20)) in $\mathcal{F}_j[j; j+m]$, in order to obtain \mathcal{F}_{j+1} . Studying the effect of transposition diamonds on homology, algorithm [38] updates a homology matrix at X_j , compatible with \mathcal{F}_j , into a homology matrix at X_{j+1} , compatible with \mathcal{F}_{j+1} defined above.

5.2 Adaptation to zigzag Morse filtrations

Using notations from Section 3, let $\overline{\mathcal{F}}$ be a general zigzag filtration:

$$\overline{\mathcal{F}} := (\emptyset =) \overline{X}_1 \xrightarrow{\Sigma_1} \overline{X}_2 \xleftarrow{\Sigma_2} \dots \xrightarrow{\Sigma_{2k-1}} \overline{X}_{2k-1} \xleftarrow{\Sigma_{2k}} \overline{X}_{2k} (= \emptyset)$$

together with Morse matchings $(\mathcal{A}_i, \mathcal{Q}_i, \mathcal{K}_i, \omega_i)$ on the set of cells Σ_i of every *forward* inclusion $\overline{X}_i \xrightarrow{\Sigma_i} \overline{X}_{i+1}$, i odd.

Let \mathcal{F} be the associated *atomic* zigzag filtration of complexes where all maps are forward or backward inclusions of a single cell: $\mathcal{F} = X_1 \longleftrightarrow \dots \longleftrightarrow X_n$.

Algorithm [38] can update a homology matrix for a general complex using reflection and transposition diamonds to implement the insertion and deletion of cells pictured in Diagrams (13). We now implement the operation of Diagram (14), introducing the chain map $\varphi_{\tau, \sigma}$.

At step j of the algorithm, we maintain a zigzag Morse filtration \mathcal{M}_j for the filtration \mathcal{F}_j . At space X_j , the filtration satisfies:

Properties 2 (Zigzag Morse filtration \mathcal{M}_j).

(1) *The filtration $\mathcal{M}_j[1; j]$ is a general zigzag Morse filtration (defined in Section 3.1) for $\mathcal{F}[1; j]$ and its Morse matchings $\{(\mathcal{A}_i, \mathcal{Q}_i, \mathcal{K}_i, \omega_i)\}_{i=1 \dots j}$,*

(2) the filtration $\mathcal{M}_j[j; j+m]$ is a standard Morse filtration (defined in [40] and Equation (8)) for the standard filtration $\mathcal{F}_j[j; j+m]$.

Before exhibiting the filtrations, we prove the following simple property of the zigzag persistence algorithm,

Lemma 8. *Let τ, σ be cells of X_j , and let $X_p \xrightarrow{\tau} X_{p+1}$ and $X_q \xrightarrow{\sigma} X_{q+1}$ be the two maps in \mathcal{F} that have the largest indices $1 \leq p, q < j$ for which a forward inclusion of τ and σ , respectively, happens in $\mathcal{F}[1; j]$.*

Let $X'_{j+r-1} \xleftarrow{\tau} X'_{j+r}$ and $X'_{j+s-1} \xleftarrow{\sigma} X'_{j+s}$, for indices $1 \leq r, s \leq m$, be the backward inclusions of τ and σ in the part $\mathcal{F}_j[j; j+m]$ of the filtration \mathcal{F}_j . Then,

$$p < q \quad \text{iff} \quad s < r.$$

In other words, if τ is inserted before σ , it is removed after σ .

Proof. The only “new” arrows in the diagram are brought by the reflection diamonds (18) applied at index j of the algorithm, on \mathcal{F}_j , which induces the desired symmetry in forward and backward arrows for the insertion of a given cell. We refer to [38] for details on the algorithm. \square

Now, consider the following diagram, where (τ, σ) are cells of X_j which are paired in the Morse matching of X_j induced by the Morse matchings $\{(\mathcal{A}_i, \mathcal{Q}_i, \mathcal{K}_i, \omega_i)\}_{i=1\dots j}$ of the filtration,

$$\begin{array}{cccccccccccccccc}
\mathcal{F}_j : & \leftarrow \cdots & X_j & \xrightarrow{\mathbb{1}} & X_j & \longleftarrow & X'_{j+1} & \longleftarrow \cdots & X'_{j+r} & \longleftarrow & X, \sigma, \tau & \xleftarrow{\sigma} & X, \tau & \xleftarrow{\tau} & X & \longleftarrow & X_{j+r-2} & \longleftarrow \cdots \\
& & \downarrow \psi_{\tau, \sigma \circ \psi} & & \downarrow \psi & & \downarrow \psi & & \downarrow \psi & & \downarrow \psi & & \downarrow \psi & & \downarrow \psi & & \downarrow \psi & & \downarrow \psi \\
\overline{\mathcal{M}}_j : & \leftarrow \cdots & \mathcal{A}_j & \xrightarrow{\varphi_{\tau, \sigma}} & \mathcal{A}_j, \sigma, \tau & \longleftarrow & \mathcal{A}'_{j+1}, \sigma, \tau & \longleftarrow \cdots & \mathcal{A}'_{j+r}, \sigma, \tau & \longleftarrow & \mathcal{A}, \sigma, \tau & \xleftarrow{\sigma} & \mathcal{A}, \tau & \xleftarrow{\tau} & \mathcal{A} & \longleftarrow & \mathcal{A}'_{j+r-2} & \longleftarrow \cdots \\
& & \downarrow \mathbb{1} & & \downarrow \psi_{\tau, \sigma} & & \downarrow \psi_{\tau, \sigma} & & \downarrow \psi_{\tau, \sigma} & & \downarrow \psi_{\tau, \sigma} & & \downarrow \psi_{\tau, \sigma} & & \downarrow \mathbb{1} & & \downarrow \mathbb{1} & & \downarrow \mathbb{1} \\
\mathcal{M}_j : & \leftarrow \cdots & \mathcal{A}_j & \longrightarrow & \mathcal{A}_j & \longleftarrow & \mathcal{A}'_{j+1} & \longleftarrow \cdots & \mathcal{A}'_{j+r} & \longleftarrow & \mathcal{A} & \longleftarrow & \mathcal{A} & \longleftarrow & \mathcal{A} & \longleftarrow & \mathcal{A}'_{j+r-2} & \longleftarrow \cdots
\end{array} \tag{21}$$

where arrows without label are simple inclusions of complexes. Simplifying notations, we denote by X the complex X'_{j+r-1} , by \mathcal{A} the complex \mathcal{A}'_{j+r-1} , and union of a complex and some cells by X, σ, τ , instead of $X \cup \{\sigma, \tau\}$. We use this diagram until the end of the section, and define its various components progressively.

Lemma 8 ensures that τ and σ , that are consecutively inserted (Morse pair, Diagram (11)), are consecutively removed in $\mathcal{F}_j[j; j+m]$, as pictured above. The filtration \mathcal{F}_j appears on top, where two arrows (curved horizontal) are further decomposed for convenience.

By induction, let \mathcal{M}_j be the zigzag Morse filtration maintained by the algorithm at step j , and satisfying Properties 2. Performing reflection diamonds (18) at index j , and transposition diamonds (20) at indices $j+r$, $r > 0$, maintains the Properties 2. Consequently, at the level of the zigzag Morse filtration, the zigzag algorithm [38] can implement insertions and deletions of critical cells (Diagrams (13)) with no further modification, while maintaining a Morse filtration $\mathcal{M}_j \mapsto \mathcal{M}_{j+1}$ satisfying the algorithmic invariant Properties 2.

The only obstruction to using the zigzag persistence algorithm is the operation introduced in Diagram (14). Consequently, consider the next operation in \mathcal{F} to be the removal $X_j \leftarrow \sigma - X_{j+1}$ of a non-critical cell σ , paired with a cell τ in the Morse matching of X_j , such that τ is not removed. The cell σ cannot be “directly removed” as it does not appear in $\mathcal{M}_j[j; j+m]$. We focus the rest of this section to the definition and study of the zigzag Morse filtration $\overline{\mathcal{M}}_j$ of Diagram (21).

Let $\overline{\mathcal{M}}_j$ be as above, where the map $\varphi_{\tau, \sigma}$ is the map defined in Diagram (14), and the chain maps ψ between \mathcal{F}_j and $\overline{\mathcal{M}}_j$ are the ones of Diagrams (13) and (14). By Theorem 6, these maps induce an isomorphism of zigzag modules $H(\mathcal{F}_j) \rightarrow H(\overline{\mathcal{M}}_j)$, and the filtrations have same persistent homology. Additionally, $\overline{\mathcal{M}}_j$ is a zigzag Morse filtration, and a standard Morse filtration from space $\mathcal{A}_j, \sigma, \tau$ on to the right, i.e., it satisfies Properties 2. Finally, σ is critical in $\mathcal{A}_j, \sigma, \tau$, and can be removed with the zigzag persistence algorithm to obtain \mathcal{M}_{j+1} .

Compatible homology matrix. We design an algorithm to turn a homology matrix at \mathcal{A}_j , compatible with \mathcal{M}_j , into a homology matrix at $\mathcal{A}_j \cup \{\tau, \sigma\}$, compatible with $\overline{\mathcal{M}}_j$, in Diagram (21).

Consider X_j in \mathcal{F}_j (Diagram (21)), containing m cells:

Definition 2 ([20]). *Let X be a cell complex of size m and $\mathcal{B} = \{c_0, \dots, c_{m-1}\}$ be a collection of m chains of $C(X)$. We say that \mathcal{B} is a homology matrix at X if there exists an ordering $\sigma_0, \dots, \sigma_{m-1}$ of the m cells of X such that:*

- (0) *for all $0 \leq r < m$, the restriction $\{\sigma_0, \dots, \sigma_r\} \subset X$ is a subcomplex of X ,*
- (1) *for all $0 \leq r < m$, the leading term of c_r is σ_r for the chosen ordering, i.e., $c_r = \varepsilon_0 \sigma_0 + \dots + \varepsilon_{r-1} \sigma_{r-1} + \sigma_r$, for some $\varepsilon_i \in \mathbb{F}$,*

and there exists a partition $\{0, \dots, m-1\} = F \sqcup G \sqcup H$, and a bijective pairing $G \leftrightarrow H$, satisfying:

- (2) *for all indices $f \in F$, $\partial^{X_j} c_f = 0$,*
- (3) *for all pairs $g \leftrightarrow h$ of $G \times H$, $\partial^{X_j} c_h = c_g$.*

This data encodes [20] the persistent homology of the (standard) filtration $\mathcal{F}_j[j; j+m]$. In particular, the homology groups of X_j are equal to $\langle [c_f] : f \in F \rangle$. It is convenient to see this data as a matrix $M_{\mathcal{B}}$ with cycle c_i as i^{th} column, expressed in the basis $\{\sigma_i\}_{i=1\dots m}$ for rows. In this case, condition (1) of the definition is equivalent to the matrix being upper triangular, with no zero entry in the diagonal.

Additionally,

Definition 3 ([38]). *We denote by $\bigoplus_{\ell} \mathbb{I}[b_{\ell}; d_{\ell}]$ the interval decomposition of $H(\mathcal{F}_j)$. A homology matrix $\mathcal{B} = \{c_0, \dots, c_{m-1}\}$ at X_j is compatible with the filtration \mathcal{F}_j iff there exists a zigzag module isomorphism $\Phi: H(\mathcal{F}) \rightarrow \bigoplus_{\ell} \mathbb{I}[b_{\ell}; d_{\ell}]$ such that $\Phi_j: H(X_j) \rightarrow \mathbb{F}^{|F|}$ sends $\{[c_f] : f \in F\}$ to the canonical basis of $\mathbb{F} \times \dots \times \mathbb{F}$.*

The Morse theory algorithm for persistent homology of [40] can be applied to maintain a compatible homology matrix for a Morse filtration under the operations pictured in Diagrams (13). We design the update for the new operation of Diagram (14). Consider:

$$\mathcal{M}_j : \mathcal{A}_1 \longleftrightarrow \dots \longleftrightarrow \mathcal{A}_j \quad \text{and} \quad \mathcal{F}_j : X_1 \longleftrightarrow \dots \longleftrightarrow X_j ,$$

such that \mathcal{M}_j is a zigzag Morse filtration for \mathcal{F}_j . Assume \mathcal{A}_j has m cells, and let $\mathcal{B} = \{c_0, \dots, c_{m-1}\}$ be a homology matrix at \mathcal{A}_j compatible with $H(\mathcal{M}_j)$. Following Diagram (14), consider:

$$\overline{\mathcal{M}}_j : \mathcal{A}_1 \leftrightarrow \dots \leftrightarrow \mathcal{A}_j \longrightarrow \mathcal{A}_j \cup \{\tau, \sigma\} \quad \text{and} \quad \overline{\mathcal{F}}_j : X_1 \leftrightarrow \dots \leftrightarrow X_j \xrightarrow{\mathbb{1}} X_j$$

such that $\overline{\mathcal{M}}_j$ is a zigzag Morse filtration for $\overline{\mathcal{F}}_j$. From \mathcal{B} , we define a homology matrix $\overline{\mathcal{B}} := \{c'_0, \dots, c'_{m-1}, c_{\tau}, c_{\sigma}\}$ at $\mathcal{A}_j \cup \{\tau, \sigma\}$ that is compatible with $H(\overline{\mathcal{M}}_j)$.

Denote the two last complexes and their boundary maps in $\overline{\mathcal{M}}_j$ by $(\mathcal{A}_j, \partial)$ and $(\mathcal{A}'_j, \partial')$, with $\mathcal{A}'_j := \mathcal{A}_j \cup \{\tau, \sigma\}$. Then:

- for all indices $i \in F \sqcup H$, define

$$c'_i := c_i - \left([\sigma : \tau]^{X_j} \right)^{-1} \left(\sum_{\nu \in c_i} [\nu : \tau]^{A'} \right) \cdot \sigma,$$

where the sum is taken over all cells ν in the support of chain c_i ,

- define $c_{\tau} := \partial' \sigma$, and $c_{\sigma} := \sigma$, and put the index of c_{τ} in G , the index of c_{σ} in H , and pair them together,
- the pairing $G \leftrightarrow H$ inherited from \mathcal{B} remains unchanged, and so does F .

Lemma 9. *The collection $\overline{\mathcal{B}}$ is a homology matrix at $\mathcal{A}_j \cup \{\tau, \sigma\}$ in Diagram (21).*

Proof. We prove that $\overline{\mathcal{B}}$ satisfies the conditions of Definition 2.

(0) Because a Morse matching induces an acyclic Hasse Diagram, there exists r such that $\sigma_0, \dots, \sigma_r, \tau, \sigma, \sigma_{r+1}, \dots, \sigma_{m-1}$ is an ordering of the cells of $\mathcal{A}_j \cup \{\tau, \sigma\}$ such that the first k cells form a subcomplex, for any k , as in Definition 2.

(1) **Case c_τ, c_σ .** The leading term of c_σ is σ . We prove that the leading term of c_τ is τ in the ordering defined above. Let \mathcal{H} be the oriented Hasse diagram of X_j for the Morse matching where (τ, σ) forms a Morse pair (complex \mathcal{A}_j), and \mathcal{H}' for the matching where τ and σ are critical (complex $\mathcal{A}_j \cup \{\tau, \sigma\}$); they differ by the orientation of arrow $\sigma \leftrightarrow \tau$. First, $\langle \partial' \sigma, \tau \rangle^{\mathcal{A}_j \cup \{\tau, \sigma\}} \neq 0$ because there exists a unique gradient path from critical cell σ to critical cell τ in $\mathcal{A}_j \cup \{\tau, \sigma\}$, which is the one edge path $\gamma = (\tau, \sigma)$. The path γ exists because τ is a facet of σ in X_j . If there were another distinct gradient path from σ to τ in \mathcal{H}' , not containing the edge $\sigma \rightarrow \tau$, this path would exist in \mathcal{H} and form a cycle with edge $\tau \rightarrow \sigma$ in \mathcal{H} ; a contradiction with the definition of Morse matchings. Second, if $\mu \in \mathcal{A}_j \cup \{\tau, \sigma\}$, is critical such that $[\sigma : \mu]^{\mathcal{A}_j \cup \{\tau, \sigma\}} \neq 0$, then μ appears before σ (and τ) in the ordering. Indeed, there exists a gradient path $\gamma = (\sigma, \mu_1, \omega(\mu_1), \dots, \omega(\mu_{r-1}), \mu_r = \mu)$ from σ to μ in \mathcal{H}' . The cells $(\mu_i, \omega(\mu_i))$ of a pair are inserted consecutively by construction, and, for all i , μ_i is inserted before $\omega(\mu_{i-1})$ because it is a facet in X_j . By transitivity, μ is inserted before σ .

Case c'_i . The leading term of c'_i is σ_i . If $c'_i = c_i$, it is direct. Otherwise, by construction, $c'_i = c_i + \alpha \cdot \sigma$, $\alpha \neq 0$, and the chain c_i contains cells ν in its support such that $[\nu : \tau]^{\mathcal{A}_j \cup \{\tau, \sigma\}} \neq 0$, i.e., cofacets of τ in $\mathcal{A}_j \cup \{\tau, \sigma\}$. With a similar transitivity argument as above, τ (and σ) must consequently appear before such ν in the ordering of cells defined. The leading term of c'_i is then unchanged.

(2) Let c_i be a chain such that $i \in F \sqcup H$. By Lemma 7, it is a direct calculation from the definition of c'_i that $\partial' c'_i = \partial c_i$. Consequently, Conditions (2) and (3) of Definition 2 are satisfied for those chains. The pairing $G \leftrightarrow H$ remains valid, because $\partial' c'_h = \partial c_h = c_g = c'_g$ for $g \leftrightarrow h$, $(g, h) \in G \times H$.

(3) By definition, $\partial' c_\sigma = c_\tau$, their indices are in $H \times G$ and paired together. \square

We now prove the compatibility condition:

Lemma 10. *The homology matrix $\overline{\mathcal{B}}$ at $\mathcal{A}_j \cup \{\tau, \sigma\}$ is compatible with $\overline{\mathcal{M}}_j$ in Diagram (21).*

Proof. By hypothesis, $\mathcal{B} = \{c_0, \dots, c_{m-1}\}$ is a homology matrix at \mathcal{A}_j , compatible with \mathcal{M}_j ; let $\Omega: H(\mathcal{M}_j) \rightarrow \oplus_{\ell} \mathbb{L}[b_\ell; d_\ell]$ be a zigzag module isomorphism such that Ω_j sends $\{[c_f] : f \in F\}$ to the canonical basis of $\mathbb{F} \times \dots \times \mathbb{F}$.

Note that, none of the c'_i have an entry τ , except for c_τ , whose index is in G by construction. Consequently, by Properties 1, the chain map $\psi_{\tau, \sigma}: C(\mathcal{A}_j, \sigma, \tau) \rightarrow C(\mathcal{A}_j)$ simply cancels the entry σ in every c'_f , $f \in F$, and $\psi_{\tau, \sigma} c'_f = c_f$. Consequently, consider the chain maps between $\overline{\mathcal{M}}_j$ and \mathcal{M}_j in Diagram (21). Each square commutes by virtue of Theorem 3 (for inclusions) and Lemma 5 (for $\varphi_{\tau, \sigma}$), and they induce an isomorphism $\Phi_*: H(\overline{\mathcal{M}}) \rightarrow H(\mathcal{M})$ of zigzag modules. The isomorphism $\Omega \circ \Phi_*: H(\overline{\mathcal{M}}) \rightarrow \oplus_{\ell} \mathbb{L}[b_\ell; d_\ell]$ sends $\{[c'_f] : f \in F\}$ to the canonical basis of $\mathbb{F} \times \dots \times \mathbb{F}$, and $\overline{\mathcal{B}}$ is compatible with $\overline{\mathcal{M}}$. \square

In conclusion, for an input atomic zigzag operation \mathcal{F} , with three atomic maps pictured in Diagrams (10), (11), and (12), the Morse algorithm for computing the zigzag persistence of \mathcal{F} is given in Algorithm 1, where the routine `zigzag_persistence_algorithm`($M_{\mathcal{B}}, \mathcal{M}_j, \sigma$) is the zigzag persistence algorithm of [38] to handle forward or backward insertions of a single cell in a homology matrix $M_{\mathcal{B}}$ at complex \mathcal{A}_j , compatible with the filtration \mathcal{M}_j (see Diagram 21). Each iteration of the `for` loop turns a homology matrix $M_{\mathcal{B}}$ at complex \mathcal{A}_j , compatible with the filtration \mathcal{M}_j , into a homology matrix at complex \mathcal{A}_{j+1} , compatible with the filtration \mathcal{M}_{j+1} , where \mathcal{M}_{j+1} is a zigzag Morse filtration for \mathcal{F}_{j+1} , and \mathcal{A}_j and \mathcal{A}_{j+1} are respectively Morse complexes for X_j and X_{j+1} .

Algorithm 1: Zigzag persistence algorithm for Morse filtrations

input : atomic zigzag filtration
 $\mathcal{F} := (\emptyset =) X_1 \longleftrightarrow X_2 \longleftrightarrow \dots \longleftrightarrow X_{n-1} \longleftrightarrow X_n (= \emptyset)$
output: persistence diagram of \mathcal{F}

```

1 set  $M_{\mathcal{B}} \leftarrow \emptyset$ ;
2 for  $j = 1 \dots n - 1$  do
3   if  $X_j \xrightarrow{\sigma} X_{j+1}$ ,  $\sigma \in X_j$  critical then
4     | use zigzag_persistence_algorithm( $M_{\mathcal{B}}$ ,  $\mathcal{M}_j$ ,  $\sigma$ ) to add or remove  $\sigma$ ;
5   end
6   if  $X_j \xleftrightarrow{\{\tau, \sigma\}} X_{j+1}$ ,  $(\tau, \sigma)$  Morse pair then
7     | do nothing;
8   end
9   if  $X_j \xrightarrow{\mathbb{1}} X_j \xleftarrow{\sigma} X_{j+1}$ ,  $\sigma$  paired with  $\tau$ ,  $\tau$  not removed then
10    | set  $M_{\mathcal{B}} \leftarrow M_{\overline{\mathcal{B}}}$  as described above;
11    | use zigzag_persistence_algorithm( $M_{\mathcal{B}}$ ,  $\overline{\mathcal{M}}_j$ ,  $\sigma$ ) to remove  $\sigma$ ;
12  end
13 end

```

Implementation and complexity. We represent $\mathcal{B} = \{c_0, \dots, c_{m-1}\}$ by an $(m \times m)$ -sparse matrix data structure $M_{\mathcal{B}}$. Assume computing boundaries and coboundaries in a Morse complex of size m is given by an oracle of complexity $\mathcal{C}(m)$. We implement the transformation $\mathcal{B} = \{c_0, \dots, c_{m-1}\} \rightarrow \overline{\mathcal{B}} = \{c'_0, \dots, c'_{m-1}, c_\tau, c_\sigma\}$ presented above by:

- computing the boundary $\partial' \sigma$ of σ in $\mathcal{A}_j \cup \{\tau, \sigma\}$, and the coboundary $\{\nu : [\nu : \tau]^{\mathcal{A}_j \cup \{\tau, \sigma\}} \neq 0\}$ of τ , in $O(\mathcal{C}(m))$ operations,
- adding columns c_τ and c_σ to the matrix in $O(m)$ operations,
- computing c'_i for all i , in $O(m^2)$. We can restrict the transformation to those c_i containing a cell of the coboundary of τ .

Consequently, we can perform the transformation above in $O(m^2 + \mathcal{C}(m))$ operations on a $(m \times m)$ -matrix. The zigzag persistence algorithm of [10, 38] deals with forward and backward insertions of a single cell in $O(m^2)$ operations.

In conclusion, let $\overline{\mathcal{F}} = (\overline{X}_i \leftarrow \Sigma_i \rightarrow \overline{X}_{i+1})_{i=1 \dots 2k}$ be a general zigzag filtration (Diagram (9)), and let \mathcal{M} be a zigzag Morse filtration as defined in Section 3, for a collection of Morse matchings $(\mathcal{A}_i, \mathcal{Q}_i, \mathcal{K}_i, \omega_i)$ on Σ_i , i odd. And:

- denote by n the total number of insertions and deletions critical cells in \mathcal{M} , and by $|\mathcal{A}_m|$ the maximal number of critical cells of a complex in \mathcal{M} ,
- denote by N the total number of insertion and deletion of cells in $\overline{\mathcal{F}}$, and by $|X_m|$ the maximal number of cells of a complex in $\overline{\mathcal{F}}$.

Additionally, we compute Morse matchings using the fast coreduction algorithm of Mrozek and Batko [42]. Even if computing optimal Morse matchings is hard in general [33], this heuristic gives experimentally very small Morse complexes, with constant amortized cost per cell considered. We compute boundaries and coboundaries in a Morse complex \mathcal{A} of a complex X by a linear traversal of the Hasse diagram of X . We store in memory the homology matrix of the Morse complex and the complex X . Consequently, the total cost of the algorithm is:

Theorem 11. *The persistent homology of $\overline{\mathcal{F}}$ can be computed in*

- *time:* $O(n \cdot |\mathcal{A}_m|^2 + n \cdot |X_m| + N)$,
- *memory:* $O(|\mathcal{A}_m|^2 + |X_m|)$.

In comparison, running the (practical) zigzag persistence algorithms [9, 10, 38] require $O(N \cdot |X_m|^2)$ operation and memory $O(|X_m|^2)$.

	Without Morse reduction				With Morse reduction			
	N $\times 10^6$	$ X_m $	time (s) cpx + pers	mem. peak (GB)	n $\times 10^6$	$ \mathcal{A}_m $	time (s) cpx + pers	mem. peak (GB)
KlBt5	63.3	187096	403 + 2912	4.7	4.9	11272	394 + 448	1.1
Spi3	66.1	47296	435 + 4438	5.2	3.8	12810	382 + 343	1.1
MoCh	75.7	37709	460 + 4680	5.8	4.1	11975	450 + 318	1.1
Sph3	99.4	66848	430 + 3498	7.5	4.2	13432	665 + 853	1.3
To3	32.8	32903	117 + 847	2.4	1.6	7570	173 + 79	0.47
By	30.5	18764	153 + 951	2.3	5.2	8677	165 + 287	0.96

Table 1: Experimental results for the oscillating Rips zigzag filtrations. For each experiment, the maximal dimension is 10, $\mu = 4$, $\nu = 6$, except for Sph3, where $\nu = 7$. The number of vertices is 2000.

6 Experiments

In this section, we report on the performance of the zigzag persistence algorithm [38] with and without Morse reduction. The corresponding code will be available in a future release of the open source library GUDHI [46].

The following tests are made on a 64-bit Linux (Ubuntu) HP machine with a 3.50 GHz Intel processor and 63 GB RAM. The programs are all implemented in C++ and compiled with optimization level `-O2` and `gcc-8`. Memory peaks are obtained via the `/usr/bin/time -f` Linux command, and timings are measured via the C++ `std::chrono::system_clock::now()` method. The timings for File IO are not included in any process time.

We run two types of experiments: homology inference from point clouds, using oscillating Rips zigzag filtrations, and levelset persistence of 3D-images. Both applications are described in the introduction.

For homology inference, we use both synthetic and real data points. The point clouds KlBt5, Spi3, Sph3, and To3 are synthetic samples of respectively the 5-dimensional Klein bottle, a 3-dimensional spiral wrapped around a torus, the 3-dimensional sphere, and the 3-dimensional torus. The point cloud MoCh and By are 3-dimensional measured samples of surface models: the MotherChild model, and the Stanford bunny model from the Stanford Computer Graphics Laboratory. The results with corresponding parameters are presented in Table 1.

Levelset persistence is computed for a function $f : [0; 1]^3 \rightarrow \mathbb{R}$, where f is a Fourier sum with random coefficients, as proposed in the DIPHA library⁴ as representative of smooth data. The cube $[0; 1]^3$ and function f are discretized into equal size voxels. For some tests, we also added random noise to the values of f . The values of $s_1 \leq s_2 \leq \dots$ are spaced out equally such that $s_{i+1} - s_i = \epsilon$ for all i . The results with corresponding parameters are presented in Table 2.

In all experiments, timings are decomposed into ‘cpx’ for computation dedicated to the complex (construction, computation of (co)boundaries and of Morse matchings) and ‘pers’ for the computation of zigzag persistence.

Analysis of the results. The results show a significant improvement when using Morse reduction. For homology inference (Table 1), the total running time is between 2.5 and 6.7 times faster when using Morse reduction. Moreover, most of the computation is transferred onto the computation of the Morse complex, which opens new roads to improvement in future implementation, such as parallelization of the Morse reduction [31] (note that parallelization of the computation of zigzag persistence is not possible in the streaming model). In particular, the computation of zigzag persistence is from 3.3 to 14.7 times faster. The better performance is due to filtrations being from 5.8 to 23.5 times shorter than the original ones (quantities n vs

⁴ github.com/DIPHA/dipha/blob/master/matlab/create_smooth_image_data.m

ϵ	max. noise	Without Morse reduction				With Morse reduction			
		$N \times 10^6$	$ X_m $	time (s) cpx + pers	mem. peak (GB)	$n \times 10^6$	$ \mathcal{A}_m $	time (s) cpx + pers	mem. peak (GB)
0.1	0	34	286780	563 + 1725	3.9	6.3	48578	224 + 29	2.7
0.15	0	-	-	∞	-	9.3	115558	756 + 44	3.6
0.15	0.5	36.5	315305	417 + 3248	4.2	4.7	36144	221 + 59	2.8
0.2	0	-	-	∞	-	15.5	245360	2097 + 68	4.7
0.2	0.5	-	-	∞	-	5.6	56500	392 + 47	3.4

Table 2: Experimental results for the level set zigzag filtrations. For each experiment, the function $f : [0; 1]^3 \rightarrow [-14, 21]$ is applied to $129^3 = 2\,146\,689$ cells and the persistence is computed for maximal dimension 3. The interval size is denoted by ϵ . The infinity symbol ∞ corresponds to more than 12 hours computing time.

N in the complexity analysis) and smaller complexes, from 2.2 to 16.6 times smaller with the Morse reduction (quantities $|\mathcal{A}_m|$ and $|X_m|$ in the complexity analysis). Note that the memory consumption with Morse reduction is from 2.4 and up to 5.6 times smaller, which is critical on complex examples in practice.

For levelset persistence (Table 2), the total running time is at least 9 times faster, and the computation of zigzag persistence alone is itself approximately 55 times faster, when the computation without Morse reduction finished. On those cases that finish, the filtration size is from 5.5 to 7.7 times shorter with Morse reduction, the maximal size of the complexes between 5.9 and 8.7 times smaller, and the memory consumption around 50% more efficient.

Additionally, using Morse reduction allows to handle cases where the standard zigzag algorithm never finishes (more than 12 hrs). On these examples, the Morse algorithm does not take more than 36 min. for the entire computation.

These results agree with the complexity analysis (Section 5) where terms $O(|\mathcal{A}_m|^2)$ and $O(|X_m|^2)$ dominate both time and memory complexities.

References

- [1] Ulrich Bauer. RIPSER: a lean c++ code for the computation of vietorisrips persistence barcodes, 2015-2016. <http://ripser.org>.
- [2] Ulrich Bauer, Michael Kerber, and Jan Reininghaus. Clear and compress: Computing persistent homology in chunks. In *TopoInVis III*, pages 103–117, 2014.
- [3] Ulrich Bauer, Michael Kerber, and Jan Reininghaus. Distributed computation of persistent homology. In *ALLENEX*, pages 31–38, 2014.
- [4] Ulrich Bauer, Michael Kerber, and Jan Reininghaus. DIPHA, a distributed persistent homology algorithm, 2014. <http://code.google.com/p/dipha>.
- [5] Ulrich Bauer and Michael Lesnick. Induced matchings and the algebraic stability of persistence barcodes. *JoCG*, 6(2):162–191, 2015.
- [6] Jean-Daniel Boissonnat, Tamal K. Dey, and Clément Maria. The compressed annotation matrix: An efficient data structure for computing persistent cohomology. *Algorithmica*, 2014.
- [7] Jean-Daniel Boissonnat, Siddharth Pritam, and Divyansh Pareek. Strong collapse for persistence. In *ESA 2018*, pages 67:1–67:13, 2018.

- [8] G. Carlsson, A. Zomorodian, A. Collins, and L. J. Guibas. Persistence barcodes for shapes. *International Journal of Shape Modeling*, 11(2):149–187, 2005.
- [9] Gunnar E. Carlsson and Vin de Silva. Zigzag persistence. *Foundations of Computational Mathematics*, 10(4):367–405, 2010.
- [10] Gunnar E. Carlsson, Vin de Silva, and Dmitriy Morozov. Zigzag persistent homology and real-valued functions. In *Symposium on Computational Geometry*, pages 247–256, 2009.
- [11] Huang-Wei Chang, Sergio Bacallado, Vijay S. Pande, and Gunnar E. Carlsson. Persistent topology and metastable state in conformational dynamics. *PLoS ONE*, 8, 04 2013.
- [12] F. Chazal, D. Cohen-Steiner, L. J. Guibas, F. Mémoli, and S. Y. Oudot. Gromov-Hausdorff stable signatures for shapes using persistence. *Proceedings of SGP*, 2009.
- [13] Frédéric Chazal, Vin de Silva, Marc Glisse, and Steve Y. Oudot. *The Structure and Stability of Persistence Modules*. Springer Briefs in Mathematics. Springer, 2016.
- [14] Frédéric Chazal, Leonidas J. Guibas, Steve Oudot, and Primoz Skraba. Persistence-based clustering in Riemannian manifolds. *J. ACM*, 60(6):41:1–41:38, November 2013.
- [15] Chao Chen and Michael Kerber. Persistent homology computation with a twist. In *Proceedings 27th European Workshop on Computational Geometry*, 2011.
- [16] Chao Chen and Michael Kerber. An output-sensitive algorithm for persistent homology. *Comput. Geom.*, 46(4):435–447, 2013.
- [17] David Cohen-Steiner, Herbert Edelsbrunner, and John Harer. Stability of persistence diagrams. *Discrete & Computational Geometry*, 37(1):103–120, 2007.
- [18] David Cohen-Steiner, Herbert Edelsbrunner, and Dmitriy Morozov. Vines and vineyards by updating persistence in linear time. In *SOCG*, pages 119–126, 2006.
- [19] Justin Curry, Robert Ghrist, and Vidit Nanda. Discrete Morse theory for computing cellular sheaf cohomology. *Foundations of Computational Mathematics*, 16(4):875–897, 2016.
- [20] Vin de Silva, Dmitriy Morozov, and Mikael Vejdemo-Johansson. Dualities in persistent (co)homology. *CoRR*, abs/1107.5665, 2011.
- [21] Vin de Silva, Dmitriy Morozov, and Mikael Vejdemo-Johansson. Persistent cohomology and circular coordinates. *Discrete & Computational Geometry*, 45(4):737–759, 2011.
- [22] O. Delgado-Friedrichs, V. Robins, and A. Sheppard. Morse theory and persistent homology for topological analysis of 3d images of complex materials. In *2014 IEEE International Conference on Image Processing (ICIP)*, pages 4872–4876, 2014.
- [23] O. Delgado-Friedrichs, V. Robins, and A. Sheppard. Skeletonization and partitioning of digital images using discrete Morse theory. *IEEE Transactions on Pattern Analysis and Machine Intelligence*, 37(3):654–666, 2015.
- [24] Olaf Delgado-Friedrichs and Vanessa Robins. Diamorse.
- [25] Pawel Dlotko and Hubert Wagner. Computing homology and persistent homology using iterated Morse decomposition. *CoRR*, abs/1210.1429, 2012.
- [26] Herbert Edelsbrunner and John Harer. *Computational Topology - an Introduction*. American Mathematical Society, 2010.
- [27] Herbert Edelsbrunner, David Letscher, and Afra Zomorodian. Topological persistence and simplification. *Discrete Comput. Geom.*, 28(4):511–533, 2002.
- [28] Emerson Escolar and Yasuaki Hiraoka. Morse reduction for zigzag persistence. *Journal of the Indonesian Mathematical Society*, 20(1):47–75, 2014.

- [29] Robin Forman. Morse theory for cell complexes. *Advances in Mathematics*, 134:90–145, 1998.
- [30] D. Gunther, J. Reininghaus, I. Hotz, and H. Wagner. Memory-efficient computation of persistent homology for 3d images using discrete Morse theory. In *2011 24th SIBGRAPI Conference on Graphics, Patterns and Images*, pages 25–32, 2011.
- [31] A. Gyulassy, P. Bremer, and V. Pascucci. Shared-Memory Parallel Computation of Morse-Smale Complexes with Improved Accuracy. *IEEE Transactions on Visualization and Computer Graphics*, 25(1):1183–1192, 2019.
- [32] Shaun Harker, Konstantin Mischaikow, Marian Mrozek, and Vidit Nanda. Discrete Morse theoretic algorithms for computing homology of complexes and maps. *Foundations of Computational Mathematics*, 14(1):151–184, 2014.
- [33] Michael Joswig and Marc E. Pfetsch. Computing optimal Morse matchings. *SIAM J. Discrete Math.*, 20(1):11–25, 2006.
- [34] Yongjin Lee, Senja Barthel, Pawe Dlotko, S. Moosavi, Kathryn Hess, and Berend Smit. Quantifying similarity of pore-geometry in nanoporous materials. *Nature Communications*, 8, 2017.
- [35] S. Lefschetz. *Algebraic Topology*. AMS books online. AMS, 1942.
- [36] Clément Maria, Jean-Daniel Boissonnat, Marc Glisse, and Mariette Yvinec. The Gudhi library: Simplicial complexes and persistent homology. In *ICMS*, 2014.
- [37] Clément Maria and Steve Oudot. Computing zigzag persistent cohomology. *CoRR*, abs/1608.06039, 2016.
- [38] Clément Maria and Steve Y. Oudot. Zigzag persistence via reflections and transpositions. In *Proceedings of SODA 2015*, pages 181–199, 2015.
- [39] Nikola Milosavljevic, Dmitriy Morozov, and Primoz Skraba. Zigzag persistent homology in matrix multiplication time. In *Symposium on Comp. Geom.*, 2011.
- [40] Konstantin Mischaikow and Vidit Nanda. Morse theory for filtrations and efficient computation of persistent homology. *Discrete & Computational Geometry*, 50(2):330–353, 2013.
- [41] Dmitriy Morozov. *Dionysus*. <http://www.mrzv.org/software/dionysus/>.
- [42] Marian Mrozek and Bogdan Batko. Coreduction homology algorithm. *Discrete & Computational Geometry*, 41(1):96–118, 2009.
- [43] Vidit Nanda. *Perseus*.
- [44] Steve Y. Oudot and Donald R. Sheehy. Zigzag Zoology: Rips Zigzags for Homology Inference. *Foundations of Computational Mathematics*, 15(5):1151–1186, 2015.
- [45] V. Robins, P. J. Wood, and A. P. Sheppard. Theory and algorithms for constructing discrete Morse complexes from grayscale digital images. *IEEE Transactions on Pattern Analysis and Machine Intelligence*, 33(8):1646–1658, 2011.
- [46] The GUDHI Project. GUDHI, 2015.
- [47] Afra Zomorodian and Gunnar E. Carlsson. Computing persistent homology. *Discrete & Computational Geometry*, 33(2):249–274, 2005.